European Journal of Pharmaceutics and Biopharmaceutics 120 (2017) 89–97

Contents lists available at ScienceDirect

European Journal of Pharmaceutics and Biopharmaceutics

journal homepage: www.elsevier.com/locate/ejpb

Research paper

Transport mechanism of chitosan-N-acetylcysteine, chitosan oligosaccharides or carboxymethyl chitosan decorated coumarin-6 loaded nanostructured lipid carriers across the rabbit ocular

Jinyu Li[a], Guoxin Tan[a], Bingchao Cheng[a], Dandan Liu[b,*], Weisan Pan[a,*]

[a] School of Pharmacy, Shenyang Pharmaceutical University, Shenyang 110016, PR China
[b] School of Biomedical & Chemical Engineering, Liaoning Institute of Science and Technology, Benxi 117004, PR China

ARTICLE INFO

Keywords:
Coumarin-6
Nanostructured lipid carrier
Chitosan-N-acetyl-L-cysteine
Chitosan oligosaccharides
Carboxymethyl chitosan
Anterior chamber drug delivery

ABSTRACT

To facilitate the hydrophobic drugs modeled by coumarin-6 (Cou-6) acrossing the cornea to the anterior chamber of the rabbit eye, chitosan (CS) derivatives including chitosan-N-acetyl-L-cysteine (CS-NAC), chitosan oligosaccharides (COS) and carboxymethyl chitosan (CMCS) modified nanostructured lipid carriers (NLCs) were designed and characterized. We found that, with similar size distribution and positive charges, different CS derivatives based on NLCs led to distinctive delivery performance. *In vivo* precorneal retention study on rabbits revealed that these CS derivatives coating exhibited a stronger resistant effect than Cou-6 eye drops and Cou-6-NLC ($P < 0.05$), moreover, the $AUC_{(0-\infty)}$, C_{max} and $MRT_{(0-\infty)}$ of them followed the sequence of CMCS-Cou-6-NLC < COS-Cou-6-NLC < CS-NAC-Cou-6-NLC. Confocal laser fluorescence microscopy (CLSM) for *in vitro* corneal penetration study showed that COS-, and CS-NAC-coated NLCs penetrated through the whole corneal epithelium barrier (about 40 μm), while CMCS failed to significantly enhance the intraocular drug penetration as expected, displayed a negligible fluorescence at 30 μm deep. In addition, penetration through the intact cornea was achieved and the penetration levels through the ocular tissues were increased thoroughly for the COS and CS-NAC coating ones compared with CMCS-NLC ($P < 0.05$), and successfully reduced the conjunctival-to-corneal permeability ratio ($ratio_{(C\text{-}S/C)}$) thus resulted in a higher bioavailability, which was confirmed by *ex vivo* fluorescence imaging on ocular tissues. In summary, CS-NAC-NLC and COS-NLC are promising ocular drug delivery systems to achieve prolonged precorneal retention, higher corneal permeability and enhanced ocular bioavailability. And comparatively speaking, CS-NAC-NLC possesses the highest potential for ocular drug delivery.

1. Introduction

Topical drug delivery is the most common treatment for diseases of the anterior segment of the eye, such as glaucoma, but it is limited by the inherent defense mechanisms in anatomical and physiological aspects. These protective functionalities are further supported by a thin lubrication film, namely tear film, which is continuously renewed by reflex lachrymation and lid blinking [1], and thus reduce the ocular bioavailability to less than 5% in spite of frequent instillations [2,3]. The situation is even worse for hydrophobic drugs, because the lower the precorneal concentration owe to the low drug solubility, the lower the concentration gradient and thus permeation through the cornea, despite the accessibility of the front of the eye [4,5]. Following the drug was administrated to the ocular surface, there are two main pathways by which the drug can enter the eye: either the corneal or conjunctival route [6]. The latter is of minor relevance for the majority of drugs and is mostly the route of absorption for biopharmaceuticals (proteins or peptides) since the conjunctiva is permeable to hydrophilic and large molecules [7]. However, the drugs that most clinical treatment used are relatively small and lipophilic. Hence, the corneal route usually dominates in ocular topical drug delivery [8]. Therefore, strategies to optimize anterior chamber drug delivery usually involve one of the following approaches: increasing drug residence time on the ocular surface by reducing lachrymal secretion and tear fluid discharge by eye closure or punctum occlusion or enhancing corneal permeability [9–11]. Worth to whistle, according to the literature, since simultaneous enhancement of the permeability of cornea and conjunctiva does not necessarily increase drug bioavailability, strategies should focus on reducing the conjunctival-to-corneal permeability ratio ($ratio_{(C-S/C)}$) [12,13].

* Corresponding authors.
E-mail addresses: liudandan1124@126.com (D. Liu), pppwwwsss@163.com (W. Pan).

http://dx.doi.org/10.1016/j.ejpb.2017.08.013
Received 8 February 2017; Received in revised form 24 August 2017; Accepted 25 August 2017
Available online 01 September 2017
0939-6411/ © 2017 Published by Elsevier B.V.

Nanostructured lipid carriers (NLCs), the second generation of SLNs, have a solid matrix blended with a liquid lipid to form a nanosized unstructured matrix. Many NLCs have shown higher drug loading capacity especially for hydrophobic drug, and reduced drug expulsion thereby, raised the local bioavailability [14,15]. However, due to the limitations of its use were the instability, anionic nature and rapid clearance of the drug from eye tissues [16], mucoadhesive polymers - like chitosan (CS) modify the NLCs was developed to obtain a better drug delivery system. In our previous studies, different CS derivatives in the form of chitosan-N-acetyl-L-cysteine (CS-NAC) (a kind of thiolated chitosan, which was synthesized in our previous study [17]), chitosan oligosaccharides (COS) and carboxymethyl chitosan (CMCS), which exhibit similar or even better biocompatibility, biodegradability, non-toxicity, mucoadhesive and permeability enhancing effect [18–22] than CS were used to modified NLCs and were conducted the mucoadhesion study *in vivo* and the corneal penetration study *in vitro* in a comparative way [17]. Interestingly, the corneal retention and the permeability enhancement of the three ocular drug delivery system were found to follow this trend: CMCS-NLC < COS-NLC < CS-NAC-NLC. However, the mechanism was mistiness, and the critical parameter of the $ratio_{(C\text{-}S/C)}$ didn't get reasonable attention. Hence, the aim of the present study was to investigate and elucidate how these different CS derivatives affected the mucoadhesion efficiency, corneal permeation and the bioavailability after coating the NLCs. For this purpose, Coumarin-6 (Cou-6), a hydrophobic fluorescence dye used as the model compound, was incorporated into the CMCS, COS and CS-NAC decorated NLCs, and the *in vivo* corneal retention and *in vitro/in vivo* corneal permeation mechanisms via an ocular topical route were investigated and compared with the conventional NLC and Cou-6 eye drops.

2. Materials and methods

2.1. Materials and animals

Coumarin-6 (Cou-6) was purchased from Aladdin® (Shanghai, China). Chitosan-N-acetyl-L-cysteine (CS-NAC, 496.7 ± 17.1 μmol/g free thiol groups) was synthesized and characterized in our previous study [17]. Chitosan oligosaccharides (COS, deacetylation degree ≥ 95%) and Carboxymethyl chitosan (CMCS, level of carboxyl ≥ 83.64%) was obtained from Aoxing Biotechnology Co., Ltd. (Zhejiang, China), and Isen Chemical Co., Ltd. (Jia Xing, China), respectively. Glyceryl monostearate (GMS), Miglyol 812 N, mixtures of caprylic/capric triglycerides and Solutol® HS15 (polyoxyl 15 hydroxystearate) was provided by BODI® chemical Holding Co., Ltd. (Tianjin, China), Sasol (Witten, Germany) and BASF (Lud-wigshafen, Germany), respectively. Gelucire 44/14 was kindly provided by Gattefosse (Paris, France). Purified water was used after deionization and filtration. All chemicals used in this study were of analytical grade or better.

Ocular damage free, male New Zealand albino rabbits (weighting 2.0–2.5 kg) were grouped by the formulations, and with six rabbits tested in each group. All animals were treated in accordance with the guidelines of Laboratory Animal Care, and the protocols were approved by the Animal Ethical Committee of the Shenyang Pharmaceutical University with the ethical committee approval number of SYPU-IACUC-C2016-0921-401.

2.2. Preparation and physicochemical characterization of the formulations

2.2.1. Preparation of formulations

Cou-6 loaded NLC was prepared by the melt-emulsification method as described in our previous report [17]. In short, aqueous phase was prepared separately by dissolving Gelucire 44/14 (1 mg/mL, 5 mL) in water and was heated to 75 °C. The formed solution was added dropwise to the uniform lipid phase (mixed under 75 °C) consisting of Cou-6 and GMS, Miglyol 812 N and Solutol®HS 15 with a mass fraction ratio of 5:112:69:89 (275 mg in total) under stirring at 600 rpm for 5 min. Ultimately, the mass ratio of the surfactant and the lipid was approximately 0.52. Then, the hot emulsion was rapidly cooled in an ice bath (0 °C) to solidify the lipid matrix and formed NLC (obtained 1 mg/mL of Cou-6-NLC).

For surface modification, 5 mL of prepared NLCs were mixed with the equal volume of 1 mg/mL each kind of polymer solutions with stirring under 600 rpm for 30 min at room temperature.

For all of the experiments, Cou-6 eye drops, the negative control, was prepared by dissolving 2.5 mg Cou-6 in 5 mL of 15% propylene glycol solution.

2.2.2. Particle characterization

The size of the NLCs were determined using photon correlation spectroscopy (PCS) and the zeta potential were measured using Laser Dopper Velocimetry (LDV) with the Zetasizer Nano ZS (Malvern Instruments Ltd., Worcestershire, U.K.). The encapsulation efficiency (EE, %) of these NLCs were calculated by determining the amount of free drug using the centrifugal ultrafiltration method and estimated by Multimode Microplate Reader (Varioskan Flash, Thermo Scientific, USA) with the excitation and the emission wavelength was 464 nm and 504 nm, respectively. The concentration of Cou-6 in these NLCs were calculated with a standard curve ($y = 716.16x + 17.60$, $R^2 = 0.9996$, x was the concentration of Cou-6 in acetonitrile solution, y was the fluorescence intensity of the samples). EE was calculated as follows:

$$EE\ (\%) = \frac{(W_{Total} - W_{Free})}{W_{Total}} \times 100 \quad (1)$$

where W_{Total}, W_{Free} were the weight of total amount of drug, amount of unwrapped drug in ultrafiltrate, respectively.

2.3. In vivo precorneal retention experiment

New Zealand albino rabbits were divided into five groups comprising six in each group randomly. The left eye of each animal received 200 μL of the samples (to maintain consistency in drug concentration, the uncoated NLC was diluted by same volume of water) containing 100 μg of Cou-6 in five instillations at 2 min intervals and closed manually for 10 s. The Cou-6 remaining on the ocular surface were collected periodically. The collections of the tear were performed by gently inserting a dry weighted filter paper strip (2 mm × 5 mm) into the lower eyelid of the rabbits and keeping the strip staying for 10 s under the eyes closed manually. The strips soaked with tear were weighted, and the weight gain pre and post-sampling were recorded to calculate the amount of tear collected. Then the strips were rinsed with 500 μL of acetonitrile and vortexes for 90 s followed by 15 min of centrifuging at 14,000 rpm for extracting Cou-6. The untreated contralateral eyes instilled with 0.9% (w/v) NaCl solution were used as control. The final supernatants were determined with Multimode Microplate Reader (*Ex/Em*: 464 nm/504 nm, Varioskan Flash, Thermo Scientific, USA), and the concentration of Cou-6 were calculated with the standard curve.

2.4. In vitro confocal laser scanning microscopy (CLSM)

In vitro permeation experiments were conducted topically on the corneas of rabbit eyes in order to track the Cou-6 from surface modified or unmodified NLCs. The enucleated eyeball was dissected within 30 min, corneoscleral buttons were dissected using standard eye bank techniques, and care was taken to minimize tissue distortion [23].

Cornea permeation studies were performed under 34 ± 0.5 °C using established procedures by mounting the rabbit corneas on Franz diffusion cell (Permegear Inc., Riegelsville, PA) with exposed area between the donor chamber and the receiver of 0.50 cm^2. The receiver compartments were filled with 4 mL of blank glutathione bicarbonate ringer buffer (GBR, pH 7.4) containing 1.2% tween 80 under magnetic stirring at 300 rpm. Accurately measured amount of samples,

equivalent to 100 μg of Cou-6, were placed in the donor cells, among which Cou-6 eye drop group was performed as the control experiment to evaluate the contribution of different CS derivatives decorating. After proceeded for 15 min or 120 min of corneal penetration experiments, the corneas were inserted into the image chamber (Coverwell™ imaging chamber, Invitrogen), and the confocal images were taken in a plane parallel to the corneal surface with a sequential scanning from 0 to 40 μm (x–y mode) with a 40× immersion objective using LAS AF Lite 2.6.0 software (Leica, Germany). Optical sections were prepared in the z-stack mode, fixing the corneal surface as the initial position. The samples were excited with a laser at 480 nm, and the fluorescence were detected at 515–530 nm. In addition, fluorescence distribution of the obtained images were analyzed by Image J in 8-bit grayscale in different corneal zones in a rabbit eye sample (n = 6). These values were also normalized by subtracting the background fluorescence recorded for the eye prior to their exposure to fluorescent nanoparticles.

2.5. Fluorescence microscopy observation of the cornea

Inverted fluorescence microscope (Olympus, BX50) was carried out to investigate the effects of CS derivatives decorated NLCs on the distribution of Cou-6 in the cornea. In this study, each dosing was divided into 5 times at 2 min intervals into the left eyes of rabbits (200 μL of formulations) and the contralateral eye was treated with normal saline as control. At the predetermined time of 15, 120, and 240 min of instillation, rabbits were euthanized by an air embolism, and the rabbit eyes were immediately enucleated. The isolated corneas dissected from the excised ocular globes were frozen at −80 °C then vertically to the sagittal with the width of 10 μm by a cryostat microtome (CM 1900, Lecia, Germany). The cornea slices were investigated under both normal light and fluorescence microscopes with Axio Cam MRm Zeiss camera at 10× magnification, exposure time 600 μs and 1388 × 1040 pixels. For the fluorescence, samples were excited with a laser at 480 nm, and the fluorescence was detected at 515–530 nm. Corneal samples without treatment were used as negative controls to configure the microscope settings. The images from the two techniques were overlaid to obtain the informations of the Cou-6 distributions in the cornea.

2.6. Ex vivo ocular distribution imaging

Cou-6-NLCs and Cou-6 eye drops (containing 100 μg of Cou-6) were instilled into the lower conjunctival sacs of each eye in rabbits to trace the distribution of different preparations within the ocular tissues. The blank eye tissues dropped with the isodose of normal saline were used as the background calibration. After sacrificed at 240 min post instillation, conjunctiva-sclera, cornea, iris-cilia and crystalline lens were separated, washed with cold saline and photographed using the FX Pro in vivo imaging system (Carestream Health, USA) equipped with an excitation at 470 nm and an emission at 535 nm.

2.7. Calculation of ocular penetration rates of Cou-6 through the ocular tissues

To calculate the ocular penetration rates of Cou-6, the dyes in the excised ocular globe or tissues were detected using Multimode Microplate Reader (*Ex/Em*: 464 nm/504 nm, Varioskan Flash, Thermo Scientific, USA). At 5 min, 30 min, 60 min, 120 min and 240 min post instillations, the rabbits were euthanized by air embolism, followed by collecting 100 μL of anterior chamber humors by inserting a 30 gage needles into the anterior chambers through the boundary between the cornea and conjunctiva. Then the excised ocular globes were carefully dissected under a microscope to produce eye segments included the cornea and conjunctival-sclera. For the ocular globes as a whole, the ocular globes were excised, and the blood was washed away by cold saline, then cut out the connective tissue. After washing with normal saline, the globe was cut into pieces carefully. Therewith, Cou-6 was extracted from the ocular globes pieces and the divided eye segments by the addition of 500 μL acetonitrile. The Cou-6 in these samples were processing with the smashing extraction method using the High-Speed Dispersator (XHF-D, Scientz, China) followed by centrifuging at 14,000 rpm for 30 min, the supernatant was collected and measured for Cou-6 content. Ocular globes and eye fragments that not treated with eye drops administration were used as controls. The ocular penetration rates of the Cou-6 after administration of various eye drops were calculated with the following formula [24]:

$$\begin{aligned} &\textit{Ocular penetration rate of dye } (\%,w/w) \\ &= (\textit{actual penetrated concentration}) \\ &\quad \div (\textit{theoretical penetrated concentration}) \times 100 \end{aligned} \tag{2}$$

where, the “actual penetrated concentration” means the real concentration of Cou-6 detected in the specimen of the ocular globe and the eye segments, the “theoretical penetrated concentration” means the virtual concentration of Cou-6 with an assumption of complete Cou-6 transition to the ocular globe after administration of various eye drops. For the ocular tissues (including the ocular globa, the cornea and the conjunctival-sclera), the theoretical penetrated concentration was 100 μg per practical mass of the eyeball. While for the aqueous humor, the theoretical penetrated concentration was 100 μg per 500 μL.

2.8. Statistical analysis

All quantitative data were expressed as the mean and standard deviation. Six samples were used for all the tests. One-way ANOVA statistical analysis was performed to evaluate the significance of the experimental data. p value < 0.05 was considered significant.

3. Results and discussion

3.1. Physicochemical characterization of the NLC

The mean particle size of the uncoated NLC was found to be 60.81 ± 0.45 nm, with zeta potential of −20.38 ± 0.39 mV. After surface modification with CMCS, COS and CS-NAC, the mean particle size of NLCs was increased to 90.04 ± 1.58 nm, 87.68 ± 3.15 and 86.74 ± 1.35 nm, and an inverted zeta potential was emerged as 14.63 ± 0.27 mV, 15.99 ± 0.32 mV and 22.50 ± 0.34 mV, respectively. Besides, CS derivatives modification showed no evident effect on the EE of NLCs as it was already up to more than 90% for the uncoated NLC. The assessment results of the particle characterization for all of the formulations used in this study were summarized in Table 1.

3.2. In vivo precorneal retention experiment

Precorneal retentional property was measured to evaluate the residence of Cou-6 in the precorneal area and to predict the potential of Cou-6 from the formulations permeated through the cornea *in vivo*. The concentration of Cou-6 from different NLC eye drops retained in the

Table 1
Evaluation of particles in the NLC eye drops (mean ± S.D., n = 6).

Samples	PS (nm)	PI	ZP (mV)	EE (%)
Cou-6-NLC	60.81 ± 0.45	0.124 ± 0.01	−20.38 ± 0.39	90.06 ± 1.82
CMCS-Cou-6-NLC	90.04 ± 1.58	0.209 ± 0.04	14.63 ± 0.27	95.28 ± 2.31
COS-Cou-6-NLC	87.68 ± 3.15	0.204 ± 0.04	15.99 ± 0.32	95.73 ± 1.87
CS-NAC-Cou-6-NLC	86.74 ± 1.35	0.196 ± 0.03	22.50 ± 0.34	96.60 ± 3.13

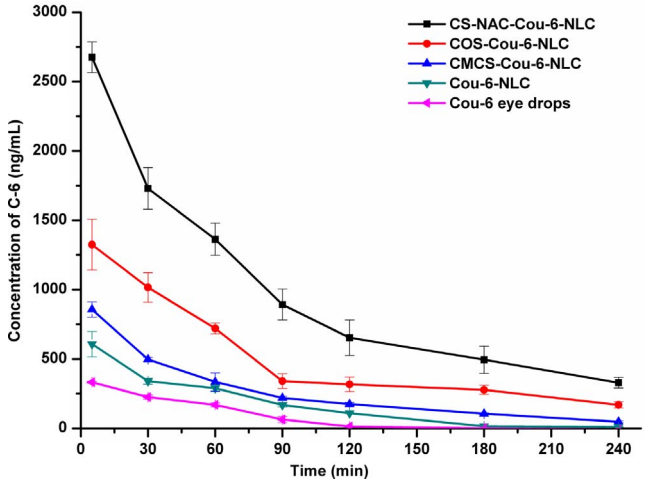

Fig. 1. The concentration-time curves of Cou-6 in rabbit tears following topical administration of the formulations (mean ± S.D., n = 6).

Table 2
Pharmacokinetic parameters of Cou-6-eye drops, Cou-6-NLC, CMCS-Cou-6-NLC, COS-Cou-6-NLC and CS-NAC-Cou-6-NLC in rabbit tears (mean ± SD, n = 6).

Samples	C_{max} (μg/mL)	$AUC_{(0-\infty)}$ (μg/mL/min)	$MRT_{(0-\infty)}$ (min)
Cou-6 eye drops	0.33 ± 0.01	19.58 ± 1.32	47.58 ± 1.11
Cou-6-NLC	0.61 ± 0.09*	40.70 ± 0.97*	64.56 ± 2.97*
CMCS-Cou-6-NLC	0.86 ± 0.05**	64.64 ± 1.35**	95.42 ± 7.86**
COS-Cou-6-NLC	1.33 ± 0.17***	146.22 ± 10.95***	178.51 ± 7.38***
CS-NAC-Cou-6-NLC	2.68 ± 0.21#	268.24 ± 11.33#	251.06 ± 6.62#

* $P < 0.05$, significant difference versus Cou-6 eye drops group.
** $P < 0.05$, significant difference versus Cou-6 NLC group.
*** $P < 0.05$, significant difference versus CMCS-Cou-6 NLC group.
# $P < 0.05$, significant difference versus COS-Cou-6 NLC group.

corneal anterior was plotted as a function of time (Fig. 1), and the pharmacokinetic parameters were presented in Table 2. For the Cou-6 eye drops group, the concentration of Cou-6 could be detected by Multimode Microplate Reader for only 120 min. Concentration of Cou-6 in unmodified NLC could be detected at the end of 180 min, whereas the concentration of Cou-6 in CS-NAC-, COS- and CMCS-coating could be detected at the end of 240 min, presenting significant corneal retention effect in rabbit eyes. According to the principle of Akaike Information Criteria (AIC) model fitting, the pharmacokinetic behaviors of these different preparations were in consistence with the single chamber model [25]. Pharmacokinetic parameters of different kinds of NLC eye drops in rabbit tears were calculated by the DAS software (V 2.0). In contrast with Cou-6 eye drops and Cou-6- NLC, the area under the curve ($AUC_{(0-\infty)}$, μg/mL/min), peak tear concentration (C_{max}, μg/mL), and mean residence time (MRT, min) of the CS derivatives coated NLCs were all increased dramatically ($P < 0.05$). Moreover, the pharmacokinetic parameters of the COS-Cou-6-NLC, and CS-NAC-Cou-6-NLC were significantly higher than CMCS-Cou-6-NLC ($P < 0.05$). These results suggested that compared to the decoration of Cou-6-NLC with COS or CS-NAC, the effect of CMCS coating was relatively wake, and this restricted effect of CMCS might owe to its moisture-absorption and moisture-retention abilities that the carboxymethyl structure endowed was time-limited [26]. Furthermore, the pharmacokinetic parameters of CS-NAC coated one was remarkably higher than the COS-Cou-6-NLC ($P < 0.05$). The prolonged residence time and the higher bioavailability of CS-NAC decoration were mainly due to its special properties. Except for the ion pairs and the hydrogen bonds effects which drive COS effect as well, CS-NAC coating were capable of forming disulphide bonds with cysteine-rich subdomains of the mucus layer which covering both corneal and conjunctival surfaces. Disulphide bonds were covalent bonds and showed stronger affinity to the binding sites and consequently facilitated a relatively long-last mucoadhesion effect [27].

3.3. Confocal laser fluorescence microscopy of the cornea epithelia

After proceeded for 15 min or 120 min of corneal penetration experiments *in vitro*, cornea samples were examined using CLSM. Fig. 2A and B depicts the acquisition of optical sections (x–y plane) taken at 0–40 μm of successive focal planes along the z axis of the corneal epithelia. Besides, the histograms of the fluorescence distribution were obtained by analyzing each image to calculate the mean fluorescence values using Image J in 8-bit grayscale (Fig. 2C and D). These values were normalized by subtracting the background fluorescence recorded for the eye prior to their exposure to the fluorescent NLCs. Assessment of coated or uncoated NLCs as well as control experiment with Cou-6 eye drops were carried out 6 times each formulation with different corneal zones in a rabbit eye samples and the results of fluorescence were calculated as the mean value (standard deviation). Fig. 2A shows that after 15 min of administration, the intense fluorescences from CS-NAC-Cou-6-NLC and COS-Cou-6-NLC treated cornea were detectable up to 40 μm of the cornea. Similarly, the fluorescence from CMCS-Cou-6-NLC was observed up to 30 μm cornea depth, while Cou-6-NLC and Cou-6 eye drop were disappeared at 20 μm cornea depth. After 120 min of penetration (Fig. 2B), an enhanced Cou-6 penetration and a more homogeneous distribution into the corneal tissue were found, and Cou-6 fluorescence were maintained until a depth of 40 μm within the corneal epithelia to both COS and CS-NAC coating. According to the literature, the thickness of the corneal epithelium of rabbits' eye is approximately 40 μm [23,28]. Therefore, it appears that COS and CS-NAC improved Cou-6 transport across the entire epithelium thickness to the beginning of the next corneal layer, the stroma. The results suggested that CMCS failed to significantly enhance the intraocular drug penetration as expected, this might attribute to its time-limited hydrogel effect and the anion effect that carboxymethyl behaves. Furthermore, CS-NAC exhibited a higher transepithelial transport than COS, and exhibits a more homogenous distribution of in deep cornea. Particularly noteworthy, in both of 15 min and 120 min (Fig. 2C and D), the gap of fluorescence intensity between COS and CS-NAC decorating were gradually increased with the depth deepening, manifested significant difference at 40 μm after 15 min instillation, and 120 min post instillation at 30 and 40 μm ($P < 0.05$). To clarify the mechanism of COS and CS-NAC coated NLCs to penetrate the corneal epithelium which might leading to this gap, the superposition of the CLSM sequence scanning fluorescence were presented as maximization (Fig. 3a and c for COS coating and CS-NAC coated ones, respectively) was taken to depicts the superficial layer of the cornea, similarly, the basal layers (40 μm, Fig. 3b and d for COS coating and CS-NAC coated ones, respectively) were presented. Apparently, for both of the two groups, at the superficial layer (Fig. 3a and c) the fluorescence of Cou-6 was observed in the cell cytoplasm and intercellular spaces and Cou-6 might have been penetrating the corneal epithelium in the form of Cou-6 molecules originating from the leaky NLC and/or in the form of intact particles. Fig. 3b and d showed some fluorescent dots which were estimated to be up to several decades of nanometers and were speculated to be the particles. While the control groups of Cou-6 eye drops and Cou-6-NLC didn't display any dot (Fig. S1, Supplementary Information). This result indicates the ability of direct particles passed through the tight junctions in the form of NLCs under the COS and CS-NAC decoration. However, by contrast, at the basal layers (40 μm, Fig. 3b and d), COS has shown just a few fluorescent dots while many visible fluorescence clusters were seen for the CS-NAC group. This could declare the difference of the mechanism between COS and CS-NAC coated NLCs to some extent, that the penetration-enhancing effect of CS-NAC was mainly attributed to the opening of the tight

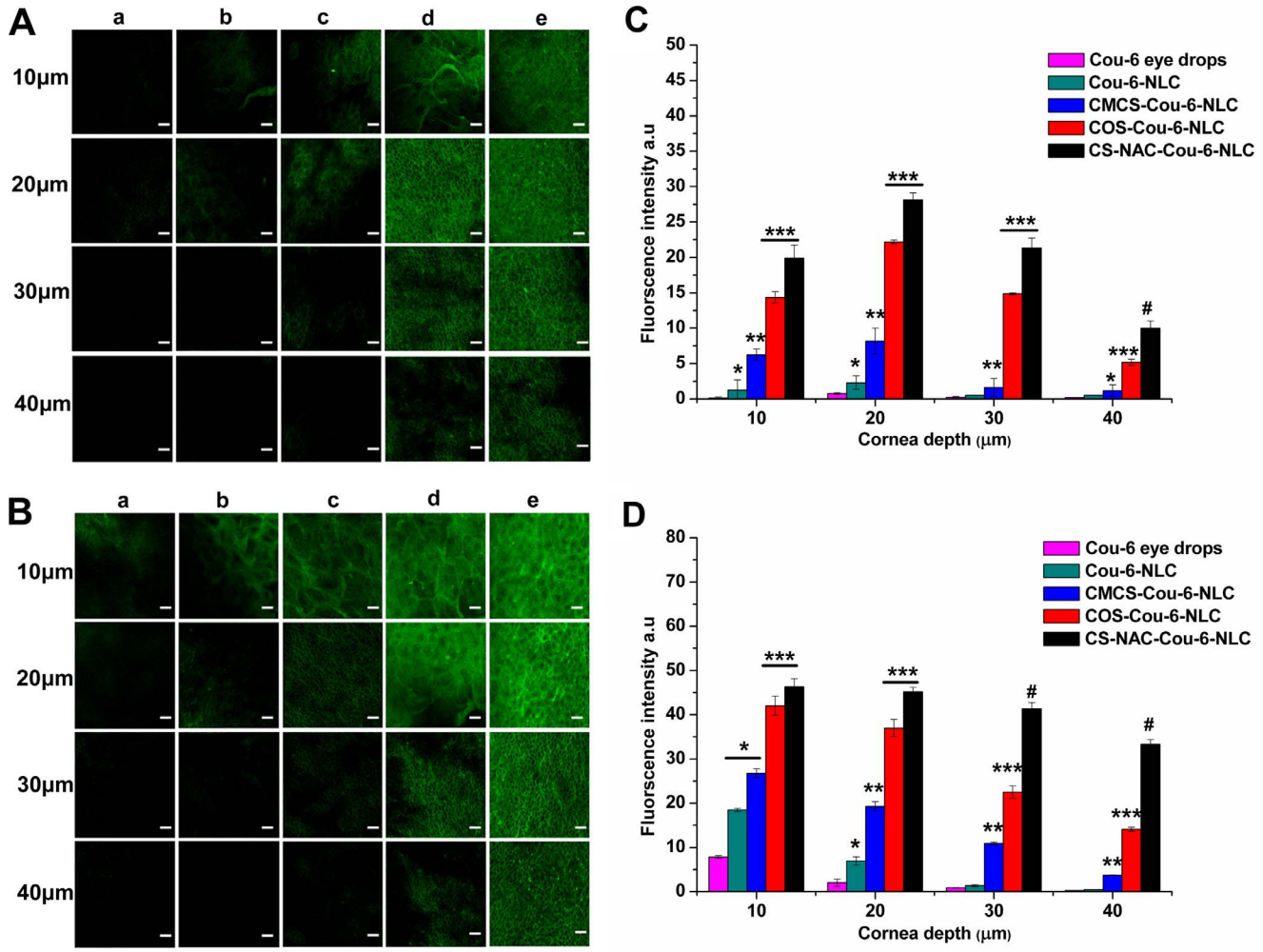

Fig. 2. Confocal laser scanning microscope for optical sections parallel to the corneal surface at different depths up to 40 μm after 15 min (A) and 120 min (B), a–e in A and B was Cou-6 eye drops, Cou-6 NLC, CMCS-Cou-6 NLC, COS-Cou-6 NLC and CS-NAC-Cou-6 NLC, respectively, scale bar is 5 μm. Comparison of the fluorescence intensity between encapsulated surface modified and unmodified NLCs after 15 min (C) and 120 min (D) (Data represent mean ± SD (n = 6); $^{*}P < 0.05$ compared to the Cou-6 eye drops group; $^{**}P < 0.05$ compared to the Cou-6 NLC group; $^{***}P < 0.05$ compared to the CMCS-Cou-6 NLC group; $^{\#}P < 0.05$ compared to the COS-Cou-6 NLC group, One way-ANOVA analysis).

junctions located between epithelial cells, resulting in an enhancement of the absorption via the paracellular route. In addition, additional intracellular pathways may contribute to the enhancement of the cellular permeability as well. For COS coating, the paracellular route and the intracellular pathway were followed by NLCs leaked inside the cytoplasm or in the space between the cells, and then entered the cell or the intercellular space of the suprabasal layer, showed a limited capacity of tight junction opening efficacy. CS-NAC-Cou-6-NLC was designed to exhibited favorable interactions with corneal epithelium mucin and the plasma membrane-associated anionic proteins, sulfated polysaccharides, or proteoglycans in coordination with the ability of opening the tight junctions, considering the thiol groups and the positive charges on the surface of the CS-NAC as well as their relatively small size. While COS was comparatively difficult to delivery the entire particles to pass through the tight functions only rely on the positive electricity and small size.

Although the Image J software could not accurately estimate the amount of Cou-6 reaching the cornea epithelia, it could evaluate the relative potency of different CS derivatives coated formulations delivered the hydrophobic Cou-6. Fig. 2C and D confirmed the results that the decoration of the COS and the CS-NAC improved Cou-6-NLC or Cou-6 penetration most significantly. By contrast, the penetration enhancing effect of CMCS coating was limited. More interestingly, at the time point of 15 min, the fluorescence intensities were reached its peak value at 20 μm cornea depth for all of the treated samples. Afterwards, the fluorescence intensities got weaken gradually in the rest of cornea depth without any strengthening phenomenon (Fig. 2C). But at 120 min post-instillation (Fig. 2D), it can be noted that the maximum levels of Cou-6 were reached at 10 μm, the first time point under evaluation, and decreased gradually over time. This might because that preparations penetrated the cornea were under the synergistic effect of mucoadhesion and penetration when in contact with the cornea. The eye surface was covered with a thin fluid layer, i.e., the so-called precorneal tear film, which has a thickness of 3–10 μm [29]. The mucin secreted in tears form a hydrophilic layer that covers the ocular surface and imparts a negative charge to the corneal and conjunctival surfaces. Thus, the preparations were trapped in the mucus and were detained at the local site of absorption and unable to distribute homogenously at the beginning 15 min. Besides, the assessments were carried out with different corneal zones in a rabbit eye samples and the results of fluorescence were calculated as a mean value (standard deviation), which could be a source of this result.

3.4. Fluorescence microscope visualization of the cornea

Inverted fluorescence microscope was used to observe the drug distribution within the cornea. The relative accumulation of fluorescence in the corneal epithelial, stroma and corneal endothelium could

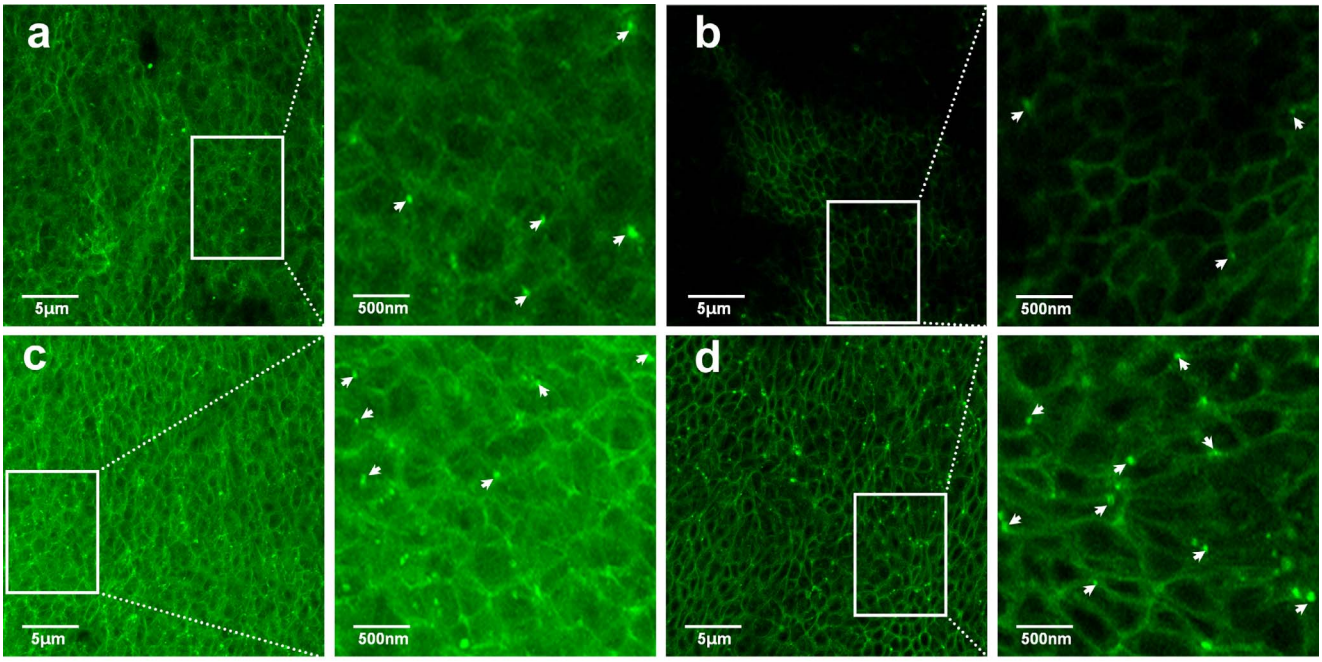

Fig. 3. Confocal laser fluorescence microscopy observation of a cornea superficial layer after treatment of COS-Cou-6-NLC and its corresponding enlarged view (a), basal layer at 40 μm and its corresponding enlarged view (b); and superficial layer after treatment of CS-NAC-Cou-6-NLC and its corresponding enlarged view (c), basal layer at 40 μm and its corresponding enlarged view (d).

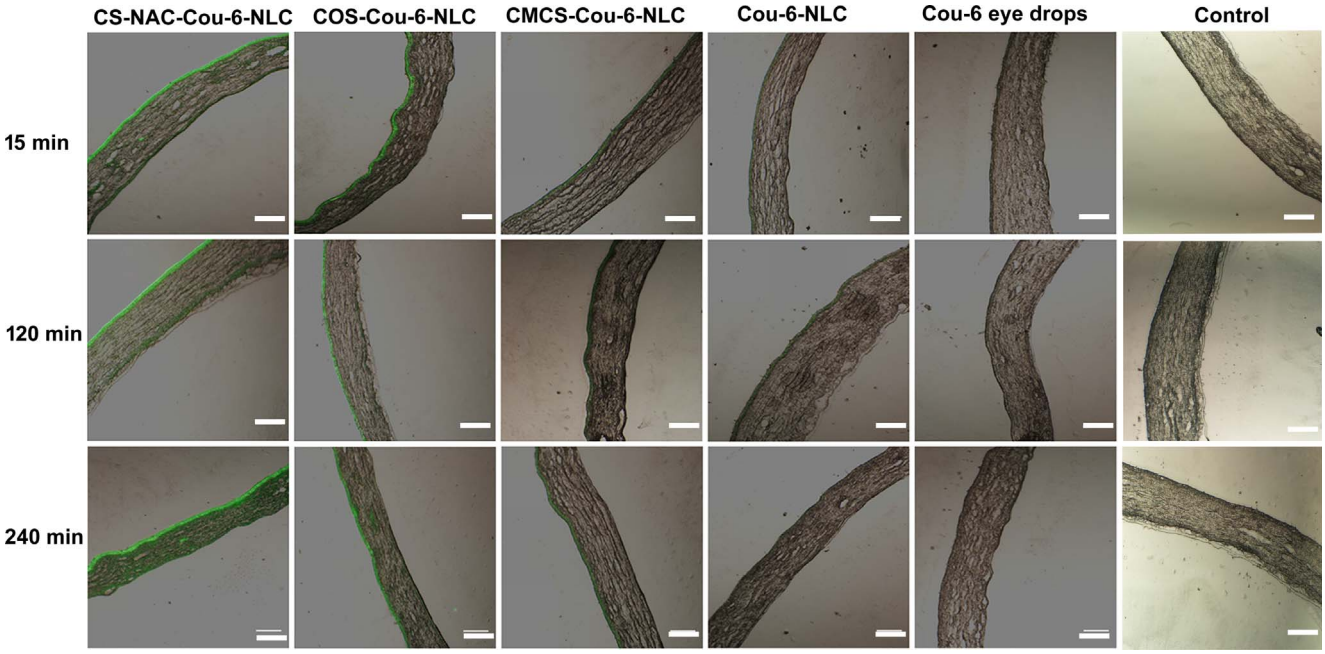

Fig. 4. Inverted fluorescence microscope micrographs after time-coursed *in vivo* corneal permeation of the preparations, the eye treated with normal saline was used as control. Scale bar is 150 μm.

be depicted in fluorescence pictures [30]. Fig. 4 depicts the overlaid normal light-fluorescence images of the cornea vertical sections after time-coursed administration of several types NLCs or eye drops. The results displayed that CS derivatives modification enhanced penetration and retention effect greatly compared with the Cou-6 eye drop group or even the uncoated Cou-6-NLC. Wherein, the NLC coated with CS-NAC showed the highest intensity of fluorescence for all time points, followed by COS-Cou-6-NLC, CMCS-Cou-6-NLC, Cou-6-NLC and Cou-6 eye drops, respectively. At the initial point of 15 min, green fluorescence could be observed for all the groups either strong or weak with the fluorescent strip of Cou-6 mainly concentrated on the corneal epithelium. At the time of 120 and 240 min the strip moved gradually into the inside of the cornea. And the green fluorescence could be observed throughout the corneal tissue in the CS-NAC coated groups after 120 min of instillation. At the time point of 240 min, the CMCS-Cou-6-NLC group showed barely intensity into the inner layer, while CS-NAC-Cou-6-NLC and COS-Cou-6-NLC exhibited deeper penetration intensity into the corneal endothelium. These results supported the assumption that drugs could permeate the cornea more effectively after incorporated into CS derivatives coated NLC and CS-NAC coating further enhanced the permeability.

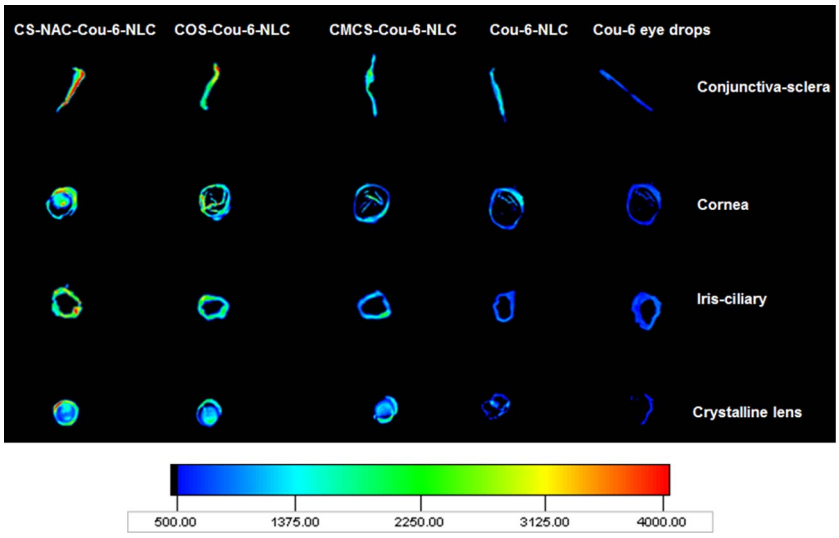

Fig. 5. *Ex vivo* fluorescence imaging of rabbit ocular tissues from rabbit treated with coated or uncoated NLCs and Cou-6 eye drops.

3.5. Ex vivo fluorescence image of rabbit ocular tissues

As demonstrated in Fig. 5, as expected, the fluorescence intensity of the conjunctiva-sclera were apparent than the cornea, and from the outside to the inside, the fluorescence intensity of the ocular tissues were gradually weakened. This implied that Cou-6 could not pass through cornea easily because of the physical barrier of cornea and conjunctiva-sclera. After the administration of uncoated Cou-6-NLC or CMCS-Cou-6-NLC, it was also observed that the fluorescence intensity of conjunctiva-sclera and cornea were enhanced modestly and the iris-cilia and crystalline lens were enhanced barely compared with the eye drops group. This finding suggested that the precorneal retention impact of Cou-6 could be improved in the form of NLC or CMCS coating NLC, but the increase of the corneal permeability were relatively difficult. Furthermore, the fluorescence intensity for both of the ocular tissues with COS or CS-NAC decorating group were enhanced significantly in comparison to the Cou-6 eye drop group or even the Cou-6-NLC group, especially the CS-NAC coating group. These findings indicated that the decoration of COS and CS-NAC could help the Cou-6-NLC through the cornea easily, resulted more Cou-6 arrived at the crystalline lens, while the CMCS failed to significantly enhance the intraocular drug penetration.

3.6. Quantitative analysis of the ocular penetration rate

Ocular penetration rates of the NLCs and Cou-6 eye drops were evaluated by quantitative analysis to measure the fluorescence intensity of prepared specimens at a given time after administration of the eye drops. The global ocular penetration rates of the various Cou-6-NLCs and Cou-6 eye drops were summarized in Table 3. The ocular penetration rates of Cou-6 through the global ocular gradually increased with time prolongs, the maximum peak penetration rates were arrived at peaking 30 min post administration for whichever preparation, and decreased thereafter. Besides, at the peaking time of 30 min after administration, uncoated NLC and CMCS, COS and CS-NAC coated NLCs improved the penetration rates of Cou-6 eye drops (0.9-, 2.13-, 4.61- and 7.85-fold) dramatically ($P < 0.05$), moreover, the decorations of the CS derivatives leading to a significant increasing effect for Cou-6-NLC ($P < 0.05$), yet the CS-NAC-Cou-6-NLC got significant higher penetration rates than COS-Cou-6-NLC ($P < 0.05$). The comparative results also revealed that the effectiveness of CMCS, COS and CS-NAC were in different level, further confirms the sequence resulted in above.

3.7. Cou-6 localization of in the ocular globe

As indicated before, when the target sites were located in the inner eye, there are two predominant pathways that drug followed [29]: the cornea and the conjunctival-sclera, and the cornea acrossed drug would firstly enter the aqueous humor and then distributed to the surrounding tissues. The concentration of Cou-6 in cornea, conjunctival-sclera and aqueous humor were illustrated as Fig. 6. In this figure, it can be noted that the maximum levels of Cou-6, in cornea and conjunctival-sclera were reached at 30 min post-instillation while the peak concentration in aqueous humor were at the time point of 60 min. The surface area of the conjunctival-sclera was approximately 17-fold larger than that of the cornea and the leaky epithelium of the conjunctival possessed more

Table 3
Ocular penetration rates (%, w/w) of the whole eye after time-coursed administration.

Types of eye drops	Time after administration of eye drops				
	5 min	30 min	60 min	120 min	240 min
	Mean value of ocular penetration rate (%, w/w)				
Cou-6 eye drops	0.454 ± 0.036	0.845 ± 0.054	0.553 ± 0.060	0.349 ± 0.024	0.254 ± 0.024
Cou-6-NLC	1.149 ± 0.089*	1.605 ± 0.105*	1.307 ± 0.049*	0.735 ± 0.080*	0.560 ± 0.058*
CMCS-Cou-6-NLC	1.507 ± 0.095**	2.647 ± 0.068**	1.793 ± 0.051**	1.120 ± 0.069**	0.838 ± 0.058**
COS-Cou-6-NLC	2.243 ± 0.107***	4.739 ± 0.257***	2.493 ± 0.266***	1.610 ± 0.110***	1.249 ± 0.137***
CS-NAC-Cou-6-NLC	3.952 ± 0.138#	7.476 ± 0.098#	5.061 ± 0.088#	2.893 ± 0.098#	2.375 ± 0.069#

* $P < 0.05$, significant difference versus Cou-6 eye drops group.
** $P < 0.05$, significant difference versus Cou-6 NLC group.
*** $P < 0.05$, significant difference versus CMCS-Cou-6-NLC group.
# $P < 0.05$, significant difference versus COS-Cou-6-NLC group.

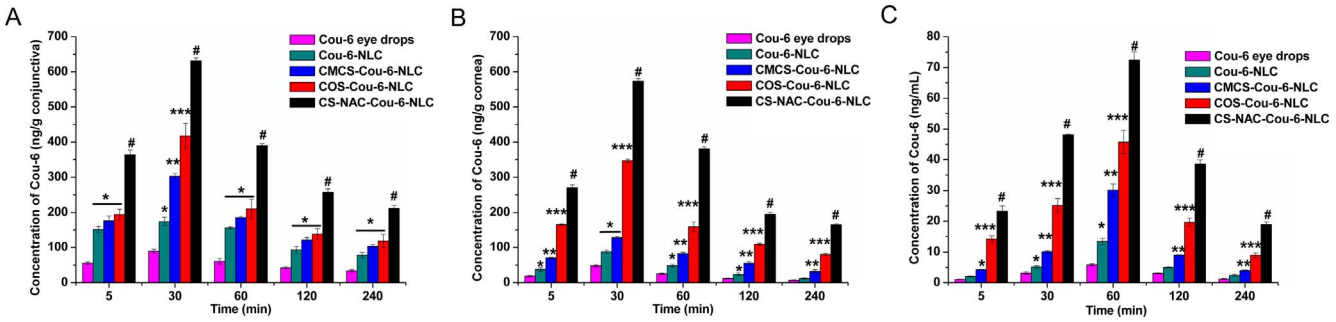

Fig. 6. Concentration of Cou-6 in ocular tissues of conjunctiva-sclera (A), cornea (B) and aqueous humor (C) at different time points (5, 30, 60, 120 and 240 min) after topical administration. Data were presented as mean ± SD (n = 6). $^{*}P < 0.05$, significant difference versus Cou-6 eye drops group, $^{**}P < 0.05$, significant difference versus Cou-6 NLC group, $^{***}P < 0.05$, significant difference versus CMCS-Cou-6-NLC group, $^{\#}P < 0.05$, significant difference versus COS-Cou-6-NLC group, One way-ANOVA analysis.

than two fold as the cornea paracellular pores [31]. Hence, if the conjunctival-sclera predominant the drug penetrated to the aqueous humor, the peak point of them should be consistent, however, this was not the case. Besides, according to the literature, the conjunctiva-sclera route did not contribute significantly as the conjunctiva-sclera area is full of blood vessels and lymphatic, which dissipate the drug into the systemic circulation or delivered the drug to the uvea and posterior tissues, but not to the aqueous humor [29,31]. While, the lag of the peaking time of Cou-6 in aqueous humor might owe to the heterogeneous nature of cornea, Cou-6 can across the corneal epithelium by transcellular either by facilitated transport or by diffusion through the paracellular pathway. After, the transport of the drug from the epithelium to the stroma may be hampered by the hydrophilic nature of the barrier, being this the main limiting step for the drug to access the inner eye. In fact, the stroma may act as a reservoir from which the drug will be slowly delivered to the aqueous humor, and this reservoir property was consistent with our previous study [17].

Furthermore, Table 4 displayed tissues permeate rates for the five formulations at 30 and 60 min post instillation, wherein, we found that through the decoration of CS derivatives, the penetrate ability of Cou-6 through the cornea, conjunctival-sclera and aqueous humor were improved significantly ($P < 0.05$) and were consistent with the sequence concluded above. However, this study and the literatures before suggest that since simultaneous enhancement of the permeability of cornea and conjunctiva does not necessarily increase drug bioavailability, strategies should focus on reducing the conjunctival-to-corneal permeability ratio ($ratio_{(C-S/C)}$) [5]. As shown in Table 4, at 30 min, the $ratio_{(C-S/C)}$ of the eye drops, NLC, CMCS-, COS-, and CS-NAC-coating were 1.87-, 1.97-, 2.36-, 1.36-, and 1.10-fold. And at 60 min, the $ratio_{(C-S/C)}$ of the eye drops, NLC, CMCS-, COS-, and CS-NAC-coating was 2.40-, 3.24-, 2.24-, 1.32-, and 1.03-fold. We can conclude that by simply packaged into NLC or CMCS-coating NLC, conjunctival absorption were increasingly favored to the detriment of corneal absorption, thereby raising the $ratio_{(C-S/C)}$ on the contrary. While, for COS and CS-NAC modified groups, although concentration in the cornea were still lower than the conjunctival-sclera, but they were approached under coating. This result further indicates that COS and CS-NAC coated NLC might be a promising approach for enhancing the permeability to the anterior segment of the eye and CS-NAC coated NLC shows more superiorities compared with COS decoration ones.

4. Conclusion

Our studies herein demonstrated that the CS derivatives including CMCS, COS and CS-NAC armed NLC led to distinctive enhancing effect on the precorneal retention and ocular penetrating performance, and followed the sequence of CMCS-, COS-, and CS-NAC-coating, in an increment trend. Besides, the corneal permeability enhancement of the coated or uncoated delivery system on drug were visualized by CLSM, confirming the modified Cou-6-NLC by COS and CS-NAC could distinct enhance the permeability of Cou-6 through the corneal epithelium by open the tight junction between epithelia cells in different degree, while CMCS failed to promote the permeability significantly, shown a negligible fluorescence at 30 μm depth of the cornea. Furthermore, visualization of the permeability into the whole cornea by fluorescence microscope and even through the cornea to anterior segment which were confirmed by *ex vivo* fluorescence image and *in vivo* distribution of different ocular tissues were conducted. As expected, COS-Cou-6-NLC and CS-NAC-Cou-6-NLC were more intensively recruited to the aqueous humor and again demonstrated their superior performance

Table 4
Ocular penetration rates (%, w/w) of Cou-6 after the administration of the five formulations at 30 min and 60 min post instillation.

Time	Types of eye drops	Time after administration of eye drops				
		Cou-6 eye drops	Cou-6-NLC	CMCS-Cou-6-NLC	COS-Cou-6-NLC	CS-NAC-Cou-6-NLC
		Mean value of ocular penetration rate (%, w/w)				
30 min	Conjunctival-sclera	0.448 ± 0.027	0.870 ± 0.061*	1.514 ± 0.039**	2.09 ± 0.18***	3.159 ± 0.041$^{\#}$
	Cornea	0.240 ± 0.016	0.442 ± 0.024*	0.641 ± 0.016**	1.534 ± 0.024***	2.871 ± 0.039$^{\#}$
	Aqueous humor	0.016 ± 0.002	0.026 ± 0.002*	0.050 ± 0.001**	0.125 ± 0.011***	0.200 ± 0.001$^{\#}$
	$ratio_{(C-S/C)}$	1.87	1.97	2.36	1.36	1.10
60 min	Conjunctival-sclera	0.305 ± 0.040	0.781 ± 0.015*	0.929 ± 0.014**	1.05 ± 0.138***	1.950 ± 0.031$^{\#}$
	Cornea	0.127 ± 0.009	0.241 ± 0.020*	0.415 ± 0.019**	0.796 ± 0.064***	1.901 ± 0.029$^{\#}$
	Aqueous humor	0.029 ± 0.002	0.067 ± 0.005*	0.150 ± 0.010**	0.229 ± 0.019***	0.362 ± 0.014$^{\#}$
	$ratio_{(C-S/C)}$	2.40	3.24	2.24	1.32	1.03

* $P < 0.05$, significant difference versus Cou-6 eye drops group.
** $P < 0.05$, significant difference versus Cou-6 NLC group.
*** $P < 0.05$, significant difference versus CMCS-Cou-6-NLC group.
$^{\#}$ $P < 0.05$, significant difference versus COS-Cou-6-NLC group.

on improving the ocular bioavailability. And by contrast, CS-NAC-NLC exhibited the highest potential for ocular drug delivery.

Acknowledgments

This work was supported by the Leading Fund of Liaoning Institute of Science and Technology (No. Yd201609), and the National Natural Science Foundation of China (81773670).

Conflict of interest

The authors have declared no conflicts of interest regarding this article.

Appendix A. Supplementary material

Supplementary data associated with this article can be found, in the online version, at http://dx.doi.org/10.1016/j.ejpb.2017.08.013.

References

[1] Y. Diebold, M. Calonge, Applications of nanoparticles in ophthalmology, Prog. Retin. Eye Res. 29 (2010) 596–609.
[2] A. Urtti, Challenges and obstacles of ocular pharmacokinetics and drug delivery, Adv. Drug Deliv. Rev. 58 (2006) 1131–1135.
[3] T. Hayashi, R. Onodera, K. Tahara, H. Takeuchi, Novel approaches for posterior segment ocular drug delivery with folate-modified liposomal formulation, Asian J. Pharm. Sci. 11 (2016) 201–202.
[4] C. Guo, F. Cui, M. Li, F. Li, X. Wu, Enhanced corneal permeation of coumarin-6 using nanoliposomes containing dipotassium glycyrrhizinate: in vitro mechanism and in vivo permeation evaluation, RSC Adv. 5 (2015) 75636–75647.
[5] W. Zhang, M.R. Prausnitz, A. Edwards, Model of transient drug diffusion across cornea, J. Control. Release 99 (2004) 241–258.
[6] E.A. Mun, P.W. Morrison, A.C. Williams, V.V. Khutoryanskiy, On the barrier properties of the cornea: a microscopy study of the penetration of fluorescently labeled nanoparticles, polymers, and sodium fluorescein, Mol. Pharm. 11 (2014) 3556–3564.
[7] Y.C. Kim, B. Chiang, X. Wu, M.R. Prausnitz, Ocular delivery of macromolecules, J. Control. Release 190 (2014) 172–181.
[8] V.P. Ranta, E. Mannermaa, K. Lummepuro, A. Subrizi, A. Laukkanen, M. Antopolsky, L. Murtomaki, M. Hornof, A. Urtti, Barrier analysis of periocular drug delivery to the posterior segment, J. Control. Release 148 (2010) 42–48.
[9] J. Jiao, Polyoxyethylated nonionic surfactants and their applications in topical ocular drug delivery, Adv. Drug Deliv. Rev. 60 (2008) 1663–1673.
[10] T. Ye, K. Yuan, W. Zhang, S. Song, F. Chen, X. Yang, S. Wang, J. Bi, W. Pan, Prodrugs incorporated into nanotechnology-based drug delivery systems for possible improvement in bioavailability of ocular drugs delivery, Asian J. Pharm. Sci. 8 (2013) 207–217.
[11] J. Iqbal, G. Shahnaz, S. Dünnhaupt, C. Müller, F. Hintzen, A. Bernkop-Schnürch, Preactivated thiomers as mucoadhesive polymers for drug delivery, Biomaterials 33 (2012) 1528–1535.
[12] D. Ghate, H.F. Edelhauser, Ocular Drug Delivery, Expert opin drug deliv. 3 (2006) 275–287.
[13] Y. Diebold, M. Jarrin, V. Saez, E.L. Carvalho, M. Orea, M. Calonge, B. Seijo, M.J. Alonso, Ocular drug delivery by liposome-chitosan nanoparticle complexes (LCS-NP), Biomaterials 28 (2007) 1553–1564.
[14] Q. Luo, J. Zhao, X. Zhang, W. Pan, Nanostructured lipid carrier (NLC) coated with chitosan oligosaccharides and its potential use in ocular drug delivery system, Int. J. Pharm. 403 (2011) 185–191.
[15] B.C. Tian, W.J. Zhang, H.M. Xu, M.X. Hao, Y.B. Liu, X.G. Yang, W.S. Pan, X.H. Liu, Further investigation of nanostructured lipid carriers as an ocular delivery system: in vivo transcorneal mechanism and in vitro release study, Colloids Surf. B: Biointerfaces 102 (2013) 251–256.
[16] J. Shen, Y. Wang, Q. Ping, Y. Xiao, X. Huang, Mucoadhesive effect of thiolated PEG stearate and its modified NLC for ocular drug delivery, J. Control. Release 137 (2009) 217–223.
[17] J. Li, D. Liu, G. Tan, Z. Zhao, X. Yang, W. Pan, A comparative study on the efficiency of chitosan-N-acetylcysteine, chitosan oligosaccharides or carboxymethyl chitosan surface modified nanostructured lipid carrier for ophthalmic delivery of curcumin, Carbohydr. Polym. 146 (2016) 435–444.
[18] A. Bernkop-Schnürch, M. Hornof, D. Guggi, Thiolated chitosans, Eur. J. Pharm. Biopharm. 57 (2004) 9–17.
[19] E. Paleček, Label-free electrochemical analysis of chitosan and glucosamine-containing oligosaccharides, Electrochim. Acta 187 (2016) 375–380.
[20] O.J. Kwon, E. Kang, J.W. Choi, S.W. Kim, C.O. Yun, Therapeutic targeting of chitosan-PEG-folate-complexed oncolytic adenovirus for active and systemic cancer gene therapy, J. Control. Release 169 (2013) 257–265.
[21] B.E. Benediktsdottir, O. Baldursson, M. Masson, Challenges in evaluation of chitosan and trimethylated chitosan (TMC) as mucosal permeation enhancers: from synthesis to in vitro application, J. Control. Release 173 (2013) 18–31.
[22] L. Casettari, L. Illum, Chitosan in nasal delivery systems for therapeutic drugs, J. Control. Release 190 (2014) 189–200.
[23] J.G. Souza, K. Dias, S.A.M. Silva, L.C.D. de Rezende, E.M. Rocha, F.S. Emery, R.F.V. Lopez, Transcorneal iontophoresis of dendrimers: PAMAM corneal penetration and dexamethasone delivery, J. Control. Release 200 (2015) 115–124.
[24] K. Baba, Y. Tanaka, A. Kubota, H. Kasai, S. Yokokura, H. Nakanishi, K. Nishida, A method for enhancing the ocular penetration of eye drops using nanoparticles of hydrolyzable dye, J. Control. Release 153 (2011) 278–287.
[25] T. Xu, J. Zhang, H. Chi, F. Cao, Multifunctional properties of organic-inorganic hybrid nanocomposites based on chitosan derivatives and layered double hydroxides for ocular drug delivery, Acta Biomater. 36 (2016) 152–163.
[26] L. Upadhyaya, J. Singh, V. Agarwal, R.P. Tewari, The implications of recent advances in carboxymethyl chitosan based targeted drug delivery and tissue engineering applications, J. Control. Release 186 (2014) 54–87.
[27] G.S. Irmukhametova, G.A. Mun, V.V. Khutoryanskiy, Thiolated mucoadhesive and PEGylated nonmucoadhesive organosilica nanoparticles from 3-Mercaptopropyltrimethoxysilane, Langmuir 27 (2011) 9551–9556.
[28] A. Ringvold, E. Anderssen, I. Kjønniksen, Impact of the environment on the mammalian corneal epithelium, Invest. Opthalmol. Vis. Sci. 44 (2003) 10.
[29] M. de la Fuente, M. Ravina, P. Paolicelli, A. Sanchez, B. Seijo, M.J. Alonso, Chitosan-based nanostructures: a delivery platform for ocular therapeutics, Adv. Drug Deliv. Rev. 62 (2010) 100–117.
[30] V. Teeranachaideekul, P. Boonme, E.B. Souto, R.H. Muller, V.B. Junyaprasert, Influence of oil content on physicochemical properties and skin distribution of Nile red-loaded NLC, J. Control. Release 128 (2008) 134–141.
[31] I. Pepic, J. Lovric, J. Filipovic-Grcic, How do polymeric micelles cross epithelial barriers, Eur. J. Pharm Sci. 50 (2013) 42–55.